Analysis of nonequidiffusive premixed flames in obstructed channels

Abdulafeez Adebiyi,[1] Olatunde Abidakun,[1] Gbolahan Idowu,[1]
Damir Valiev,[2] and V'yacheslav Akkerman[1,*]
[1]*Center for Innovation in Gas Research and Utilization (CIGRU), Center for Alternative Fuels, Engines and Emissions (CAFEE), Computational Fluid Dynamics and Applied Multi-Physics Center, Department of Mechanical and Aerospace Engineering, West Virginia University, Morgantown, West Virginia 26506, USA*
[2]*Center for Combustion Energy, Key Laboratory for Thermal Science and Power Engineering of Ministry of Education, Department of Energy and Power Engineering, Tsinghua University, Beijing 100084, China*

(Received 27 December 2018; published 11 June 2019)

The impact of the Lewis number, Le, on the dynamics and morphology of a premixed flame front, spreading through a toothbrushlike array of obstacles in a semiopen channel, is studied by means of the computational simulations of the reacting flow equations including fully compressible hydrodynamics and one-step Arrhenius chemical kinetics. The channels of blockage ratios $\alpha = 1/3,\ 1/2,\ 2/3$ are considered, with the Lewis numbers in the range $0.2 \leqslant \mathrm{Le} \leqslant 2$ employed. It is shown that the Lewis number influences flame evolution substantially. Specifically, flame acceleration weakens for $\mathrm{Le} > 1$, inherent to fuel-rich hydrogen or fuel-lean propane burning. In contrast, $\mathrm{Le} < 1$ flames, corresponding to lean hydrogen-air or rich propane-air mixtures, acquire strong folding of the front and thereby accelerate even faster. The latter effect can be devoted to the onset of the diffusional-thermal combustion instability.

DOI: 10.1103/PhysRevFluids.4.063201

I. INTRODUCTION

Flame acceleration (FA) and a deflagration-to-detonation transition (DDT) are often considered within the context of fire safety, but they are also expected to be relevant in improving various advanced combustion technologies such as pulse-detonation engines [1] or microcombustors [2]. FA caused by the flame response to small perturbations or curvature is oftentimes affected by the elongation and thickening of the flame front, as a thickened flame front offers higher resistance to corrugation and, thereby, to acceleration [3,4].

Among geometries associated with FA and DDT, obstructed pipes provide the fastest regime of burning [5]. While flame propagation through obstacles [6,7] is oftentimes associated with turbulence, shocks [8], or hydraulic resistance [9], Bychkov *et al.* [10–13] have identified and scrutinized a conceptually laminar, shockless mechanism of ultrafast FA in semiopen channels or tubes equipped with a toothbrushlike array of obstacles. This mechanism is illustrated in Fig. 1, and it is associated with a powerful jet-flow formation along the channel centerline, generated by a cumulative effect of delayed combustion in the pockets between the obstacles, which causes outflow of a newly generated volume of expanding burning matter from the side pockets into the free central part of the channel. The burnt gas moves towards the unobstructed part of the channel from opposing pockets, with gas flow velocity changing predominantly to the axial direction, resulting in strong

*Corresponding author: West Virginia University, Morgantown, WV 26506-6106; vyacheslav.akkerman@mail.wvu.edu

forward push of the leading flame tip. More pockets are formed and ignited due to propagation of the flame tip, and accumulation of burnt gases coming out from these pockets causes even higher acceleration. This feedback loop of pocket ignition, burnt gas expansion, and FA may result in a detonation onset, provided the channel is long enough.

According to the analytical formulation [10], substantiated by the computational simulations [10,11,13], a flame accelerates in a two-dimensional (2D) obstructed channel as

$$\frac{U_{\mathrm{tip}}}{S_L} = \Theta \exp\left[\frac{(\Theta - 1)}{(1-\alpha)}\frac{S_L}{R}t\right] = \Theta \exp(\sigma\tau), \quad \sigma = \frac{(\Theta - 1)}{(1-\alpha)}, \tag{1}$$

where $U_{\mathrm{tip}} \equiv dZ_{\mathrm{tip}}/dt$ is the flame tip velocity in the laboratory reference frame; S_L the planar flame speed; $\Theta \equiv \rho_u/\rho_b$ the thermal expansion in the burning process; R the half width of the channel; $\alpha = h/R$ the blockage ratio, with h being the obstacle height; and $\tau = S_L t/R$ the scaled time. This FA is extremely powerful indeed: say, for typical $\Theta = 8$ and $\alpha = 1/2$, the scaled exponential acceleration rate of Eq. (1) is $\sigma = (\Theta - 1)/(1-\alpha) = 14$, which is much larger than the scaled acceleration rates due to wall friction [14] being of the order of unity. It is noted that for obstacles-based acceleration, the quantity σ drastically depends on α; it grows with α and Θ, thereby promoting FA, but it does not depend on R. To some extent, this makes the Bychkov acceleration mechanism Reynolds independent and, thereby, relevant to various scales, including microcombustors, and industrial conduits, as well as mining and subway tunnels.

The theory and modeling [10] adopted a set of simplifications, including a conventional approach of equidiffusive combustion, when the Lewis number Le, defined as the thermal-to-mass diffusivities ratio, is unity, $\mathrm{Le} = 1$. However, $\mathrm{Le} \neq 1$ often in practice, which leads to the interplay between the internal and global flame structures such as the diffusional-thermal instability. The impact of Le on FA has been found substantial in the narrow *unobstructed* channels [15–18]. Specifically, it has been shown that FA in unobstructed channels is drastically promoted in the $\mathrm{Le} < 1$ premixtures, due to enormous extra elongation of the flame front [17]. In contrast, $\mathrm{Le} > 1$ combustion leads to a thicker flame front, thereby moderating FA.

May we expect the same or similar impacts of Le in the obstructed channels? Answering this question constitutes the focus of the present work. Frankly speaking, the authors did not expect such a strong impact of Le in the obstructed geometry as in the unobstructed one, because it was suspected that the obstacles would prevent a strong elongation of the flame wings. However, despite such an intuitive expectation, we have found that the role of Le is significant in the obstructed conduits, with moderation of FA for the $\mathrm{Le} > 1$ flames and strong promotion of acceleration in the case of $\mathrm{Le} < 1$. In fact, the impact of the Lewis number is found to be as strong as that of the blockage ratio α.

This paper is structured as follows: the governing equations, numerical methodology, and description of the computational platform are presented in Sec. II, while Sec. III shows the results of the numerical simulations and discussions. The paper is concluded with a brief summary.

II. NUMERICAL METHOD

We performed the computational simulations of the following 2D set of equations:

$$\frac{\partial}{\partial t}\rho + \frac{\partial}{\partial x_i}(\rho u_i) = 0, \quad \frac{\partial}{\partial t}(\rho u_i) + \frac{\partial}{\partial x_j}(\rho u_i u_j + \delta_{ij}P - \gamma_{i,j}) = 0, \tag{2}$$

$$\frac{\partial}{\partial t}\left(\rho e + \frac{1}{2}\rho u_i u_j\right) + \frac{\partial}{\partial x_i}\left(\rho u_i h + \frac{1}{2}\rho u_i u_j u_j + q_i - u_j\gamma_{i,j}\right) = 0, \tag{3}$$

$$\frac{\partial}{\partial t}(\rho Y) + \frac{\partial}{\partial x_i}\left(\rho u_i Y - \frac{\zeta}{Sc}\frac{\partial Y}{\partial x_i}\right) = -\frac{\rho Y}{\tau_R}\exp(-E_a/R_p T), \tag{4}$$

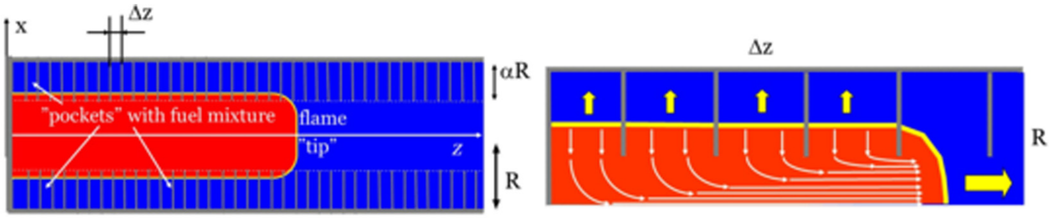

FIG. 1. An illustration of the Bychkov mechanism of flame acceleration in an obstructed channel [10–13].

where Y is the mass fraction of the fuel mixture; $e = QY + C_v T$ and $h = QY + C_p T$ are the specific internal energy and enthalpy, respectively; $Q = C_p T_f(\Theta - 1)$ is the energy release in the reaction, with the specific heat at constant volume, C_v, and pressure, C_p, the initial fuel temperature, $T_f =$ 300 K; pressure, $P_f = 1$ bar; and density $\rho_f = 1.16\ \mathrm{kg/m^3}$. The stress tensor $\gamma_{i,j}$ and the energy diffusion vector q_i read

$$\gamma_{i,j} = \zeta\left(\frac{\partial u_i}{\partial x_j} + \frac{\partial u_j}{\partial x_i} - \frac{2}{3}\frac{\partial u_k}{\partial x_k}\delta_{i,j}\right), \quad q_i = -\zeta\left(\frac{C_p}{\mathrm{Pr}}\frac{\partial T}{\partial x_i} + \frac{Q}{\mathrm{Sc}}\frac{\partial Y}{\partial x_i}\right), \tag{5}$$

where $\zeta = \rho\nu$ is the dynamic viscosity, being $\zeta_f = 1.7 \times 10^{-5}\ \mathrm{kg/(m\,s)}$ in the fuel mixture, with Sc and Pr being the Schmidt and Prandtl numbers, respectively, such that the Lewis number has been determined as their ratio, $\mathrm{Le} = \mathrm{Sc}/\mathrm{Pr}$. In the present work, we vary Le by changing Sc while the Prandtl number is kept constant, $\mathrm{Pr} = 1$. The flame thickness can be defined, conventionally, as $L_f \equiv \zeta_f/\rho_f S_L \mathrm{Pr} = 4.22 \times 10^{-5}$ m. As a result, Eqs. (2)–(5) include the fully compressible hydrodynamics, transport properties (heat conduction, diffusion, and viscosity), and chemistry modeled by a single irreversible Arrhenius reaction of the first order, with the activation energy E_a and the constant of time dimension τ_R. More details of the numerical scheme and the solver can be found, for instance, in Refs. [10,11,13].

Similar to Fig. 1, a flame propagates in a long 2D channel of width $2R$, where a fraction $2R\alpha$ is blocked by the obstacles with spacing (the distance between two neighboring obstacles) Δz. The channel width is described by the Reynolds number associated with flame propagation, $\mathrm{Re} \equiv RS_L/\nu = R/L_f\mathrm{Pr} = R/L_f$. In the present work, we used $\Delta z = R/4$; $R/L_f = 24,\ 36,\ 48$; and $\alpha = 1/3,\ 1/2,\ 2/3$. The walls of the channel and the obstacles are adiabatic, $\mathbf{n}\cdot\nabla T = 0$, and free slip, $\mathbf{n}\cdot\mathbf{u} = 0$, where $\mathbf{n}$ is the normal vector at the wall. The absorbing (nonreflecting) boundary conditions are employed at the open end to prevent the reflection of the sound waves and weak shocks. The left end of the free part of the channel is closed while the other end, on the right, is open, with the boundary conditions $\rho = \rho_f$, $P = P_f$, and $u_z = 0$ adopted. The initial flame structure is imitated by the Zeldovich-Frank-Kamenetskii-like solution for a hemispherical flame front [19],

$$T = T_f + (T_b - T_f)\exp\left(\left[-\sqrt{(x^2+z^2)} + r_f\right]/L_f\right) \quad \text{if} \quad z^2 + x^2 \geqslant r_f^2, \tag{6}$$

$$T = \Theta T_f \quad \text{if} \quad z^2 + x^2 < r_f^2, \tag{7}$$

TABLE I. Resolution test.

$\Delta z_f/L_f$	$U_{w,\max}/U_f$	$\Delta U_{w,\max}/U_f$	Z_{tip}/R	$\lvert\Delta Z_{\mathrm{tip}}/R\rvert$
0.4	2.9143		1.8667	
0.2	2.9345	0.0202	1.9583	0.0916
0.1	2.9431	0.0086	1.9208	0.0375

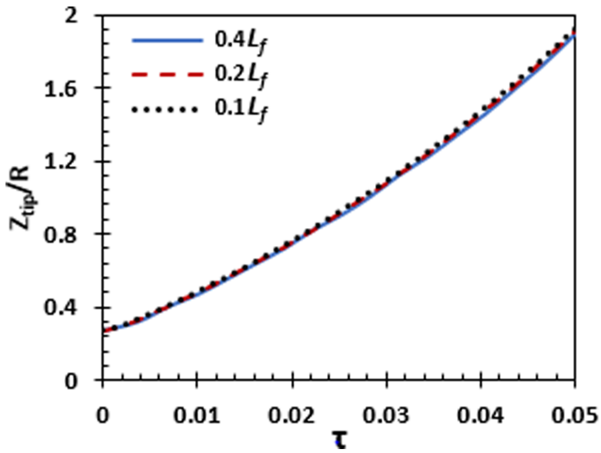

FIG. 2. Resolution test: The scaled flame time position versus the scaled time for $\alpha = 1/3$, Le $= 0.2$, and various square mesh sizes: $(0.1, 0.2, 0.4)L_f$.

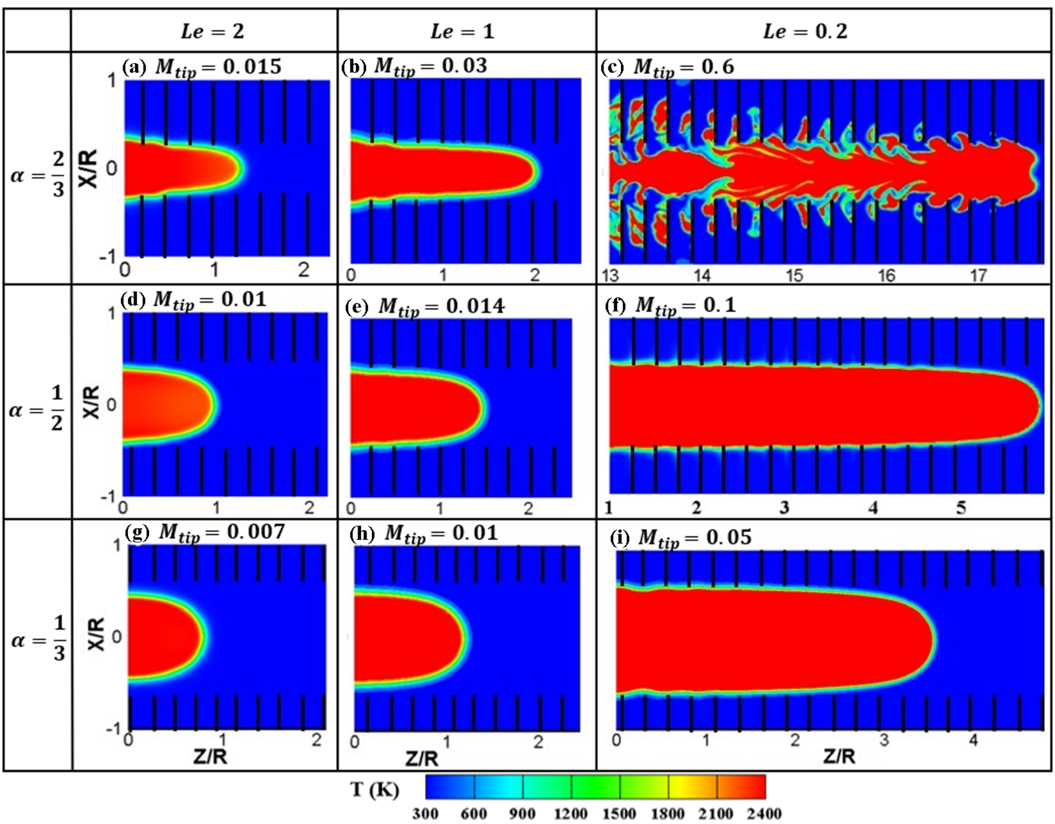

FIG. 3. Temperature snapshots taken at the same scaled time instant $\tau = S_L t/R = 0.075$ for various $\alpha = 1/3$, $1/2$, and $2/3$ and various Le $= 0.2, 1.0, 2.0$.

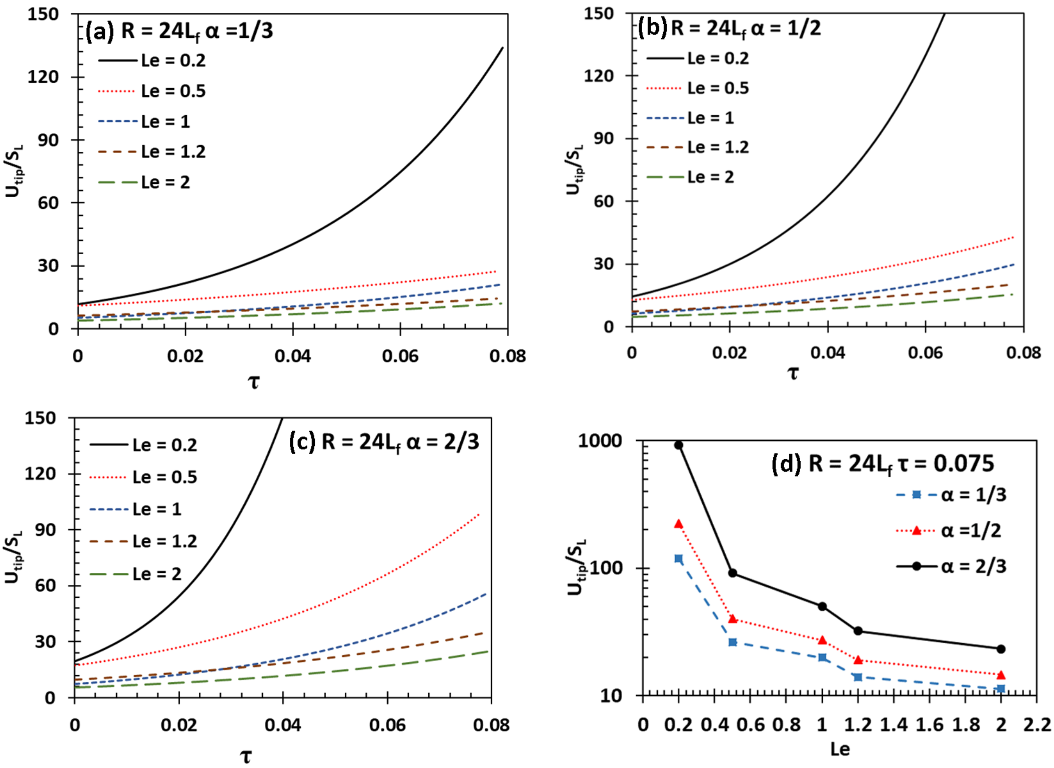

FIG. 4. The scaled flame tip velocity $U_{\rm tip}/S_L$ versus the scaled time τ for $R/L_f = 24$ and $\alpha = 1/3$ (a), $1/2$ (b), $2/3$ (c). Panel (d) shows the scaled flame tip velocity $U_{\rm tip}/S_L$ at $\tau = 0.075$ versus Le for different values of $\alpha = 1/3, 1/2, 2/3$.

ignited at the centerline, and the closed end of the channel, with an initial radius $r_f = 5.1L_f$, with

$$Y = (\Theta - T/T_f)/(\Theta - 1), \quad P = P_f, \quad u_x = 0, \quad u_z = 0\,, \tag{8}$$

such that $Y = 0$ in the burnt matter and $Y = 1$ in the fresh fuel mixture.

A square grid of size $0.2\,L_f$ (the spatial resolution validated earlier for equidiffusive flames [11]) was adopted in the present work. We also performed a resolution test for nonequidiffusive flames with $\mathrm{Le} = 0.2$ by conducting and comparing the simulation runs with the square meshes of sizes $0.1\,L_f$, $0.2\,L_f$, and $0.4\,L_f$. As shown in Table I and Fig. 2, for $R/L_f = 24$ and $\alpha = 1/3$, the results converge such that the mesh of size $0.2\,L_f$ adequately resolves the flame front even for the Lewis numbers much less than unity.

Both the fuel mixture and burnt matter are assumed to be ideal gases of constant molecular weight, $M = 29$ kg/kmol, such that the equation of state is $P = \rho R_p T/M$ with the universal gas constant $R_p = 8.314$ J/mol K. The chemical properties of the fuel mixture are chosen to model methane-air burning with a Lewis number in the range $0.2 \leqslant \mathrm{Le} \leqslant 2.0$, thermal expansion coefficient $\Theta = 8$, and the planar flame speed $S_L = 34.7$ cm/s. The initial speed of sound in this fuel mixture is 10^3 times larger, $c_0 = 347$ m/s, such that hydrodynamics is almost incompressible at the initial stage of burning. In this respect, in addition to the standard scaling of Eq. (1), $U_{\rm tip}/S_L$, we also scaled $U_{\rm tip}$ by the local, instantaneous speed of sound $c_{\rm tip} = \sqrt{(c_p/c_v) \times (R_p/M) \times T_{\rm tip}}$. Such a flame tip Mach number $M_{\rm tip}(t) = U_{\rm tip}/c_{\rm tip}$ appears to be a good measure of the instantaneous level

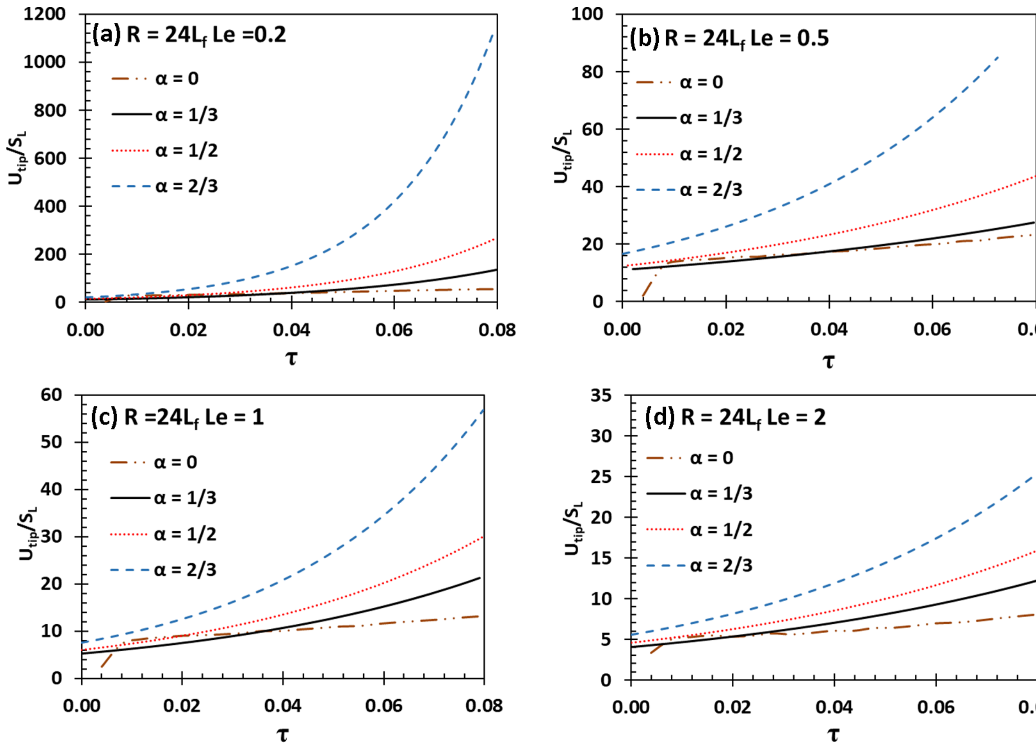

FIG. 5. The scaled flame tip velocity $U_{\rm tip}/S_L$ versus the scaled time τ for $R/L_f = 24$ and various Le = 0.2 (a), 0.5 (b), 1.0 (c), 2.0 (d).

of compressibility as well as of the instantaneous stage of the DDT process, being $M_{\rm tip} \ll 1$ at the initial, quasi-isobaric stage of burning and approaching an order of unity by the time of detonation triggering.

III. RESULTS AND DISCUSSION

We have performed extensive computational simulations of premixed FA in the configuration described above, and for various Lewis numbers, blockage ratios, and flame propagation Reynolds numbers. Figures 3(a)–3(i) show the flame shapes and positions attained at various Le, Le = 0.2, 1.0, 2.0; and α, $\alpha = 1/3,\ 1/2,\ 2/3$ at the same time instant, $\tau = S_L t/R = 0.075$, and for the same $R/L_f = 24$ in all nine simulation runs. The respective $M_{\rm tip}|_{\tau=0.075}$ are also depicted. The flames are represented by the temperature snapshots, with a temperature ranging from 300 K in the fuel until 2400 K in the burnt matter. It is seen that the role of the Lewis number is paramount and as strong as that of the blockage ratio. Indeed, when both the effects of large α and nonequidiffusivity (with Le < 1) work together, as in Fig. 3(c) for $\alpha = 2/3$ and Le = 0.2, then the flame front is drastically folded, having propagated over considerable distance, with the flame tip Mach number as high as $M_{\rm tip} = 0.6$. In contrast, a Le > 1 flame in a channel with small blockage ratio accelerates very slowly, as observed in Fig. 3(g) for $\alpha = 1/3$ and Le = 2.0. In other cases of Fig. 3, the effects of α and Le on flame acceleration compete, such that almost equivalent flame structures and $M_{\rm tip}$ are observed in the pairs of Figs. 3(d) and 3(h); 3(a) and 3(e); and even 3(b) and 3(i).

To quantify the impact of Le, in Fig. 4 we present the time evolution of the scaled flame tip velocity, $U_{\rm tip}/S_L$, for several blockage ratios, $\alpha = 1/3$ [4(a)], $1/2$ [4(b)], and $2/3$ [4(c)], with various

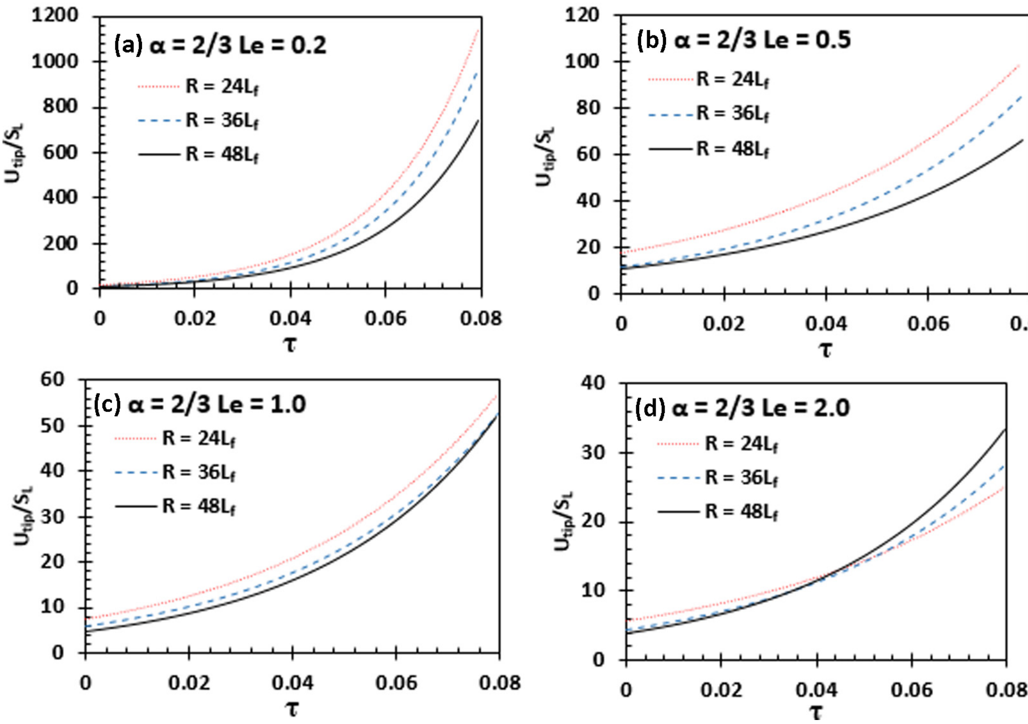

FIG. 6. The scaled flame tip velocity U_{tip}/S_L versus the scaled time τ for $\alpha = 2/3$ and various Le = 0.2 (a), 0.5 (b), 1.0 (c), 2.0 (d).

Le, Le $= 0.2,\ 0.5,\ 1.0,\ 1.2,\ 2.0$ in each plot. It is seen that the effect of Le is very strong, especially for the Le < 1 flames. Indeed, in all three of Figs. 4(a)–4(c), Le $= 0.2$ leads to an increase in U_{tip} almost by an order of magnitude as compared to the equidiffusive case, Le $= 1$. The effect of Le $>$ 1 is substantially weaker, but Le $= 2.0$, nevertheless, noticeably moderates FA as compared to the Le $= 1$ cases. Figure 4(d) depicts the variation of the logarithm of scaled tip velocity with Le at $R/L_f = 24$ and the scaled time instant $\tau = 0.075$ (similar to Fig. 3). It is shown that the flame velocity increases as Le decreases for all values of α, with the greatest increase observed at Le < 1, and minimal changes at Le above unity.

Figure 5 illustrates the role of the blockage ratio α in the acceleration of the flame tip. It is seen that the α dependence is significant and much stronger than the Re dependence for all the Lewis numbers considered. At the same time, the impact of Le on the α dependence is smaller than that on the Re dependence: namely, the α dependence does not change sign due to Le, but there is a noticeable quantitative effect such that the α dependence is stronger for the Le < 1 flames. For various Le, the flames exhibit weaker acceleration in unobstructed channels, $\alpha = 0$, as compared to that in obstructed ones. In fact, in the case of $\alpha = 0$ we arrive to the classical finger flame acceleration scenario [20,21]. According to Ref. [13], there exists a critical blockage ratio α at which the obstacles-based acceleration mechanism is replaced by finger flame acceleration.

Figure 6 scrutinizes the role of a channel width for various Le and α. It is seen that the impact of R is minor as all the curves for $R/L_f = 24,\ 36,\ 48$ in Figs. 6(a)–6(d) attain very similar acceleration rates (the derivatives of the curves seen). This supports the Bychkov formulation [10] predicting Re-independent FA, Eq. (1). On the other hand, Fig. 6 shows a very intriguing result: the impact of Le modifies the Re-dependence up to the opposite one. Indeed, FA weakens with Re for the Le $\leqslant 1$

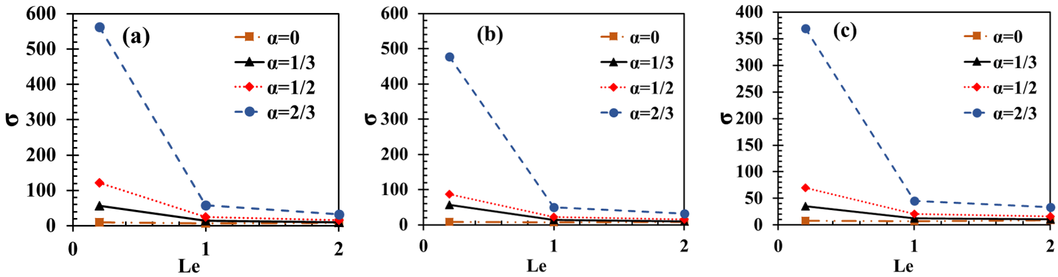

FIG. 7. The exponential acceleration rate σ versus the Lewis number Le for $R/L_f = 24$ (a), 36 (b), and 48 (c), with $\alpha = 1/3$, $1/2$, and $2/3$ in each panel.

flames due to decreasing flame stretch, Figs. 6(a)–6(c), but it is promoted with Re in the Le > 1 case for the opposite reason, Fig. 6(d). In this light, we can potentially look for a certain threshold Le that would correspond to the change of the trend and thus provide the complete Re-independence. While adiabatic walls are assumed here, it is, however, important to note that heat losses at the walls may modify the flow behind the flame front, thereby influencing the dynamics of the flame tip.

Finally, the acceleration trends were analyzed, and in the cases when the exponential trends are exhibited, $Z_{\text{tip}} \propto \exp(\sigma\tau)$, the exponential acceleration rate σ was estimated as the slope from the semilogarithmic plot of the scaled flame tip position Z_{tip}/R versus scaled time $\tau = S_L t/R$. The resulting σ is plotted versus Le in Fig. 7, for $R/L_f = 24,\ 36,$ and 48 in Figs. 7(a)–7(c), respectively, with $\alpha = 1/3$, $1/2$, and $2/3$ in each figure. The acceleration rate σ is largest for the nonequidiffusive cases of Le < 1. Also, in order to unify the analysis, similar to Bychkov *et al.* [10], the combination $\sigma Z_{\text{tip}}/\Theta R$ is plotted versus $\sigma S_L t/R$ in Fig. 8 [it is recalled that $\sigma = (\Theta - 1)/(1 - \alpha)$; see Eq. (1)]. While Ref. [10] was limited to equidiffusive flames, Le = 1, with all data collapsing into a single curve, here we have various Le, and the set of curves associated with different Le differ. However, for each given Le, the plots collapse into a single curve, consistent with the Bychkov model.

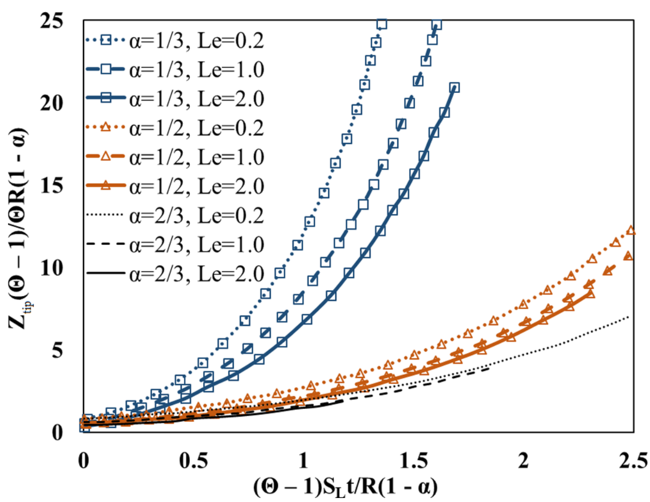

FIG. 8. The scaled flame tip position $\sigma Z_{\text{tip}}/\Theta R$ versus the scaled time $\sigma t S_L/R$ for various Le = 0.2 (dotted), 1.0 (dashed), and 2.0 (solid), with three different $\alpha = 1/3$ (square markers), $1/2$ (triangle markers), and $2/3$ (without markers) for each given Le.

IV. CONCLUSIONS

In this work, a thorough investigation of FA in obstructed channels has been performed for nonequidiffusive fuel mixtures, by means of computational simulations, and a profound impact of the Lewis number Le on FA has been identified. This effect is compared to that of the blockage ratio α and it has been found to be as strong. In the case of Le < 1, promotion of FA is discovered. It is found that the Lewis number has an influence on the α dependence. In contrast, moderation of FA has been observed for Le > 1 flames. In addition, a unique trend is noticed for the Le impact on a Re dependence. Indeed, the Lewis number may change a Re-dependence of FA to an opposite trend.

ACKNOWLEDGMENTS

The work at West Virginia University was sponsored by the US National Science Foundation (NSF), through CAREER Award No. 1554254 (V.A.), as well as by the West Virginia Higher Education Policy Commission, through Grant No. HEPC.dsr.18.7 (V.A.). The work at Tsinghua University was supported by the National Natural Science Foundation of China (NSFC), through Grant No. 51750110503, and by the Thousand Young Talents Plan program.

[1] G. Roy, S. Frolov, A. Borisov, and D. Netzer, Pulse detonation propulsion: Challenges, current status, and future perspective, Prog. Energy Combust. Sci. **30**, 545 (2004).

[2] Y. Ju and K. Maruta, Microscale combustion: Technology development and fundamental research, Prog. Energy Combust. Sci. **37**, 669 (2011).

[3] N. Chakraborty and R. S. Cant, Physical insight and modelling for Lewis number effects on turbulent heat and mass transport in turbulent premixed flames, Numer. Heat Transfer, Part A **55**, 762 (2009).

[4] H. Xiao, J. Sun, and X. He, A study on the dynamic behavior of premixed propane-air flames propagating in a curved combustion chamber, Fuel **228**, 342 (2018).

[5] E. S. Oran and V. N. Gamezo, Origins of the deflagration-to-detonation transition in gas-phase combustion, Combust. Flame **148**, 4 (2007).

[6] C. Wang, X. Dong, J. Cao, and J. Ning, Experimental investigation of flame acceleration and deflagration-to-detonation transition characteristics using coal gas and air mixture, Combust. Sci. Technol. **187**, 1805 (2015).

[7] B. Zhang, H. Liu, and C. Wang, On the detonation propagation behavior in hydrogen-oxygen mixture under the effect of spiral obstacles, Int. J. Hydrogen Energy **42**, 21392 (2017).

[8] G. Ciccarelli and S. Dorofeev, Flame acceleration and transition to detonation in ducts, Prog. Energy Combust. Sci. **34**, 499 (2008).

[9] I. Brailovsky, L. Kagan, and G. Sivashinsky, Combustion waves in hydraulically resisted systems, Philos. Trans. R. Soc., A **370**, 625 (2012).

[10] V. Bychkov, D. Valiev, and L.-E. Eriksson, Physical Mechanism of Ultrafast Flame Acceleration, Phys. Rev. Lett. **101**, 164501 (2008).

[11] D. Valiev, V. Bychkov, V. Akkerman, C. K. Law, and L.-E. Eriksson, Flame acceleration in channels with obstacles in the deflagration-to-detonation transition, Combust. Flame **157**, 1012 (2010).

[12] V. Bychkov, V. Akkerman, D. Valiev, and C. K. Law, Influence of gas compression on flame acceleration in channels with obstacles, Combust. Flame **157**, 2008 (2010).

[13] O. Ugarte, V. Bychkov, J. Sadek, D. Valiev, and V. Akkerman, Critical role of blockage ratio for flame acceleration in channels with tightly spaced obstacles, Phys. Fluids **28**, 093602 (2016).

[14] V. Bychkov, A. Petchenko, V. Akkerman, and L. Eriksson, Theory and modelling of accelerating flames in tubes, Phys. Rev. E **72**, 046307 (2005).

[15] J. B. Bell, R. K. Cheng, M. S. Day, and I. G. Shepherd, Numerical simulation of Lewis number effects on lean premixed turbulent flames, Proc. Combust. Inst. **31**, 1309 (2007).

[16] C. Cui, M. Matalon, and T. L. Jackson, Pulsating mode of flame propagation in two-dimensional channels, AIAA J. **43**, 1284 (2005).

[17] V. Akkerman, S. Bilgili, V. Bychkov, D. Valiev, S. Demir, and H. Morella, Impacts of the Lewis and Markstein numbers effects on flame acceleration in channels, in *40th Technical Meeting of the Eastern States Section of the Combustion Institute, ESSCI 2016* (Eastern States Section of the Combustion Institute, NJ, USA, 2016).

[18] D. Fernandez-Galisteo, C. Jimenez, M. Sanchez-Sanz, and V. N. Kurdyumov, Effects of stoichiometry on premixed flames propagating in narrow channels: Symmetry-breaking bifurcations, Combust. Theory Modell. **21**, 1050 (2017).

[19] C. K. Law, *Combustion Physics* (Cambridge University Press, New York, 2006).

[20] C. Clanet and G. Searby. On the 'tulip flame' phenomenon, Combust. Flame **105**, 225 (1996).

[21] V. Bychkov, V. Akkerman, G. Fru, A. Petchenko, and L.-E. Eriksson, Flame acceleration in the early stages of burning in tubes, Combust. Flame **150**, 263 (2007).